Structure of the proposed RI biosensor (sensor with two functions)

Abderraouf HOCINI[1,*], Assia DAAS[1], Abdesselam HOCINI[2], Souheil MOUETSI[1]

[1] Department of Electrical Engineering, Faculty of Sciences and Applied Sciences,Pole Ain Beida, University of Oum El Bouaghi, 04201. Algeria.
[2] Laboratoire d'Analyse des Signaux et Systèmes, Department of Electronics, University of M'Sila BP.166, Route Ichebilia, M'Sila, 28000, Algeria.

*Email: raoufho28@gmail.com hocini.abderraouf@univ-oeb.dz

Abstract. Photonic sensors, in light of proposed structures comprised of rhombus–molded gaps matched with two waveguides, have been developed as another enthusiasm for specialists in science and technology. In this paper, it has been demonstrated that by utilizing the rhombus–formed openings examination, they got outcomes which are brilliant inside the depression locale. Consequently, the quality factor (Q) and the affectability (S) can be essentially improved for the proposed structure. This investigation are performed by reproduction utilizing limited contrast time area (FDTD). Different affectability are acquired as 565.38 nm/RIU and quality factor as high as 2.61×10^{5}have been accomplished, deducing in a location breaking points 1.03×10^{-6}. This blend angle gives the proposed structure an extra exhibition as a component to play out a name free biosensing for the biomedical visualization.

1. Introduction

Optical sensors, that offer prompt revelation and measurement of organic investigation, have pulled in an extraordinary consideration owing to their promising highlights, for example, security in a burnable and hazardous environment, assurance from electromagnetic impedances, snappy reaction and the separated web based detecting capacity. Photonic gems (PhC) are occasional dielectric components with the capacity to screen and control light age and stream. The periodicity can be shaped by embedded and punctured openings in a dielectric component, making a photonic band hole (PBG) area [1–2]. PhC have been utilized in few applications, as in twist waveguides, channels, sensitizers, lasers, amplifiers, and resonators. Among those optical innovations, receptive photonic precious stone (PhC) built sensors have gotten a lot of consideration because of their microcosmic size, their high affectability, negligible model preparing denied of fluorescence classifying and the chance of participate in MEMS (Micro Electro-Mechanical Systems) [3]. More often than not, it is about physical and compound/biochemical challenges, the PhC sensors offer an incredibly solid narrow mindedness inside the substance to be broke down, because of the effect of the photonic taboo band [4].The light can be packed in an extremely little volume, communicating with a colossal fluid light [5]. This wonder leaves the sensors to be very sensitive to minor refractive list (IR) factors that are shaped by the natural medium, with limits on the dividers of the PhC test. The examination is completed continuously and doesn't require the utilization of markers (bio-location without name). The acquired discoveries can be improved via doing advancements in the sensor frameworks, for instance a warmth balance, the movement of the coupling and the topological streamlining of the geometry (shape, opening size, thickness and Si level). At this premise, an assortment of IR sensor proposition have been broken down and acknowledged by means of various sorts of PhC structures, for example, smaller scale depressions [6-7-8], waveguides [9-10], Slotted waveguides [11-12-13-14], hetero-structures [15], from which critical advancements in detecting stages have been arranged. A large portion of these arranged sensors work as a solitary thought or sensor and the quantity of brands that can be veiled on one event is very

little. So, as to ease this lack, the fundamental thought is to build up a framework to permit blending a few research thoughts on a colossal substrate. That is the reason PhC-based sensors have been imagined and tried. A few photonic gem topologies have been proposed in the writing for structure of biosensors, contrasted and photonic precious stone smaller scale hole which has more deformity modes and optical restriction impact. So, as to improve the affectability of photonic precious stone miniaturized scale hole sensor, it is important to propose a sensor structure with colossal optical confinement impact [16-17-18-19].

In this paper, we depict the system and the reproduction procedure of the proposed PhC biosensor that is speculatively utilized for evaluating the glucose's focus. Considering the silicon-on-encasing (SOI) innovation, the planned structure is molded by two waveguides with ring-formed openings pit framework. The detecting standard depends on the move of reverberation frequency λ0, which occurs because of the adjustment in RI of the sensor when the PhC's air gaps are involved by a homogenous demonized water (n = 1.33) or other fluid (distilled water n = 1.3147, methanol n = 1.316, acetone n = 1.3445, isopropyl alcohol n = 1.363 [20]).For the glucose recognition, it has been affirmed that the resounding frequency design changes its unearthly position following a direct demonstration when the glucose fixation somewhere in the range of 0% and 60% is applied. The properties of the sensor are reproduced utilizing the limited distinction time-space (FDTD) calculation (RSoft CAD). In theory and statistics, light concentration in photonic crystals is estimated by resolving Maxwell's calculations in a varied dielectric medium, stated in equations (1)and (2); E and H are the electric and magnetic field intensities.

$$\nabla\times E(r,t)=-\frac{\partial}{\partial t}\left[\mu_0.H(r,t)\right] \quad (1)$$

$$\nabla\times H(r,t)=-\frac{\partial}{\partial t}\left[\varepsilon.\varepsilon_0(r).E(r,t)\right] \quad (2)$$

μ is the permeability which equals to μ0 as the measured material is non-magnetic,
ε :symbolizes the permittivity which is habitually written as $\varepsilon=\varepsilon_0.\varepsilon(r)$, where ε_0 is the permittivity of vacuum and ε(r) is the relative permittivity of the material.

Equation (3) is obtained by solving Equation (1) and inserting it into the time derivative of Equation (2):

$$\nabla\times\left[\frac{1}{\varepsilon(r)}\nabla\times H(r,t)\right]=-\frac{\partial^2}{\partial t}\left[\mu_0.H(r,t)\right] \quad (3)$$

Assuming harmonic time dependence for the magnetic field with angular frequency ω. $H(r, t) = H(r)\, e^{-i\omega t}$, we obtain the master equation for the magnetic field:

$$\nabla\times\left[\frac{1}{\varepsilon(\vec{r})}\nabla\times H(\vec{r})\right]=\left(\frac{\omega}{c}\right)^2 H(\vec{r}) \quad (4)$$

The spatial and temporal steps are related through this equation:

$$\Delta t\leq\frac{1}{c}\left(\Delta x^{-2}+\Delta y^{-2}\right)^{1/2} \quad (5)$$

Where c is the speed of light in vacuum,
Δx and Δy are spatial stages in the *x*and *y*directions, respectively.

In order to terminate the computational field, the perfectly matched layers (PMLs) are employed [21].

2. Materials and theoretical model

The proposed plan depends on a 2D-PhC structure. It comprises of a periodical triangular grid of air-expanded gaps punctured in a silicon (Si) piece (refractive list n_{si}=3.45).The range of the air openings is r=0.38a, with a cross section steady a=550 nm, the thickness of the PhC chunk is set as h=230 nm. The Silicon dioxide (SiO_2) layer with a thickness of 1500 nm and low refractive record is utilized as a supporting layer to the high filed Silicon based chunk, to keep light to the pit center, forestalling optical misfortunes in the lower substrate, and the light detainment in the vertical course is then protected by full interior reflection. So as to

diminish the computational time which may happen in 3D structures, the PhC is changed into a 2D framework with the dielectric medium having the viable refractive file of 2.868, which relates to the powerful file of the focal guided TE mode. For the accompanied numerical reenactments, we have applied the powerful file approach given in [22], in blend with two different techniques specifically the 2D-PWE and the 2D-FDTD from the RSoftprogramming bundle. The dispersal properties of the deliberate PhC structure have been investigated utilizing the 2D-PWE technique in Band SOLVE programming. For the TE polarization, the photonic band hole (PBG) covers the scope of ω_1=0.278(a/λ) to ω_2=0.4 (a/λ) comparing to the wide frequency goes of1323.7>λ>1908.1 nm.

Subsequently, the viable working frequency extend is adequate to satisfy the detecting need, where the full mode creates a wide frequency move. Figure 1 shows the schematic of the planned biosensor. This last comprises of two waveguide couplers and one cavity. The two waveguides are acquired by expelling one column of air-expanded gaps in the x course, to couple light source in and out the Silicon section punctured ring-molded gaps PhC depression.

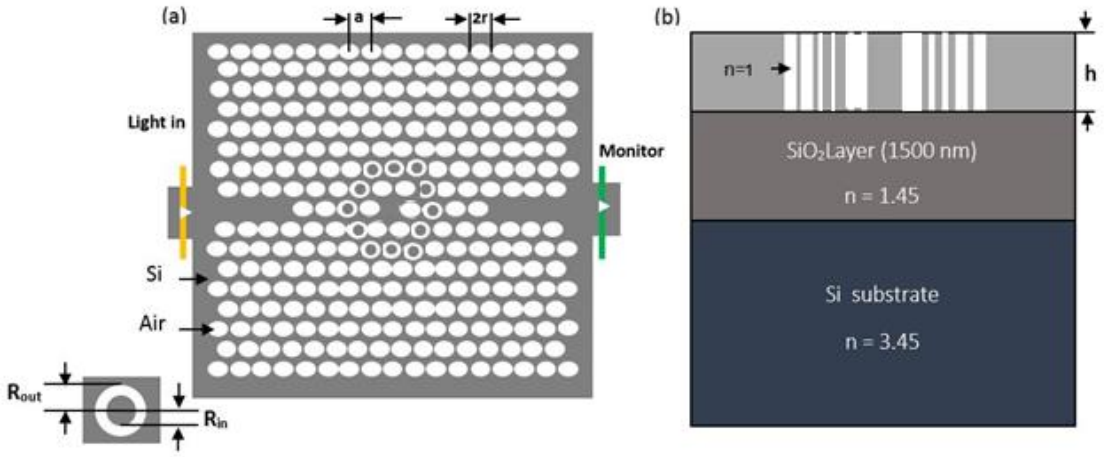

Figure 1. (a) Schematic diagram of the proposed rhombus-shaped photonic crystalcavity coupled to an input and output the PC waveguides.
(b)Schematic side and sectional view of the proposed PC biosensor structure in SOI substrate.

It is important to note that the ring-formed gaps arrangement doesn't just give greater adaptability as far as planning new structures in correlation with to roundabout molded ones, but also to improve the optical field containment, thus light-liquid cooperation inside the ring of low-dielectric material territory [23-24].

The ring-formed gap parameters are characterized by their internal and external range Rin=121nm (0.22a) and Rout=247.5 nm (0.45a) individually.In this manner the ringed air-expanded district is given by Rout−Rin=126.5 nm. The entire depression framework is isolated from the info and yield waveguides by three PhC gaps.

Two-dimensional limited contrast time-area (2D-FDTD) technique is utilized to gauge the structure's usefulness, considering the Perfect Matched Layers (PML) conditions in computations, to guarantee no back appearance in the broke down locale's breaking point.

In reproduction process, a TE energized Gaussian optical heartbeat, covering the entire recurrence scope of intrigue, is propelled at the information port to energize the hole modes. A force screen was put toward the finish of the yield waveguide to gauge the transmitted sign, and to improve the reproduction's precision, FDTD investigation is completed with a lattice size of0.01 nm.

3. Sensing properties of the designed structure

So, for showing the working head of the PhC pit based RI biosensor, a progression of FDTD reproductions have been led. The starter detecting examination is finished by assuming the neighborhood penetration of de-ionized (DI) water in the hole detecting zone, this compares to the change in refractive file (RI) of the ring molded gaps from 1.33 (DI-water) to 1.332305450 of (0 g/l to 60 g/l).

The relation between both the glucose's RI n and concentration C, can be expressed as follows [25]:

$$n = 0.00011889.C + 1.33230545 \quad (6)$$

For a neighborhood invasion, an exact system dependent on small scale penetration innovation by means of empty submicron size pipettes has been tentatively shown in [26]. This strategy permits to control a fluid affidavit inside an ideal PhC gap, and not influencing the nearby ones.

For assessing the usefulness of the structure, for instance fluid, should be in contact with the sensor, and the reproduction is done by changing the RI of the gaps from 1.3147 (refined water) to 1.363 (isopropyl liquor). This prompts a move in the yield transmission range that relates to an adjustment in the RI.

Figure 2, the quality factor, sensitivity and transmission spectrum of resonant mode will change with N .

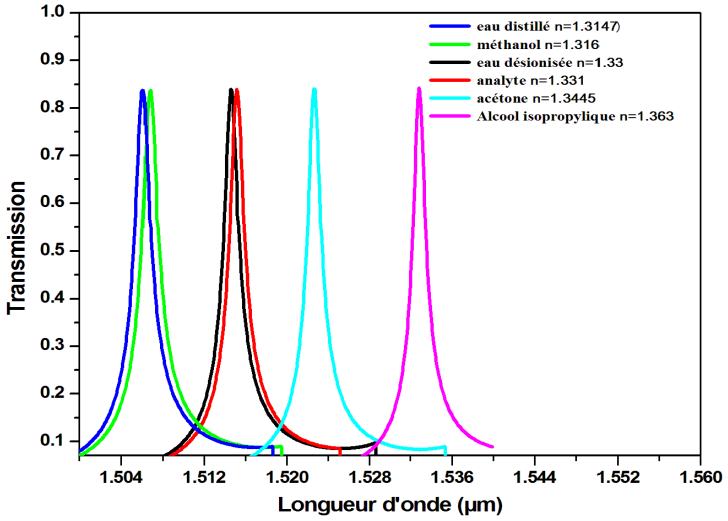

Figure 2. Transmission spectra.

Normalized transmission spectrum of the PC cavity as a function of wavelength is also illustrated in figure 2. According to changing the RI of the gaps from 1.3147 (refined water) to 1.363 (isopropyl liquor). we can find that the normalized transmittance remains the same and can reach to 84.5. It can be seen in this figure that when the number of functionalized holes increases, the resonant wavelength shifts to ward larger amounts. Figure 2is in their lower values, which can explain the choice of the local infiltration instead of the total infiltration.

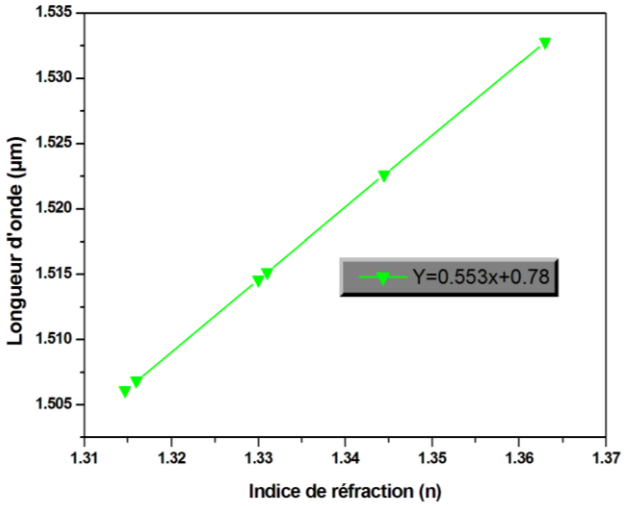

Figure 3. Resonant wavelength shift as a function of the RI n.

From figure 3, and if we assume that the relationship between the resonance shift and the refractive index is approximately linear,equation7 describes the resonance displacement for a given liquid index to predict the resonant frequency after a linear fit of the simulation data:

$$Y[\mu m] = (0.553.x + 0.78)[\mu m] \quad (7)$$

The quality factor of the proposed structures are calculated for different refractive indices as shown in the following figure:

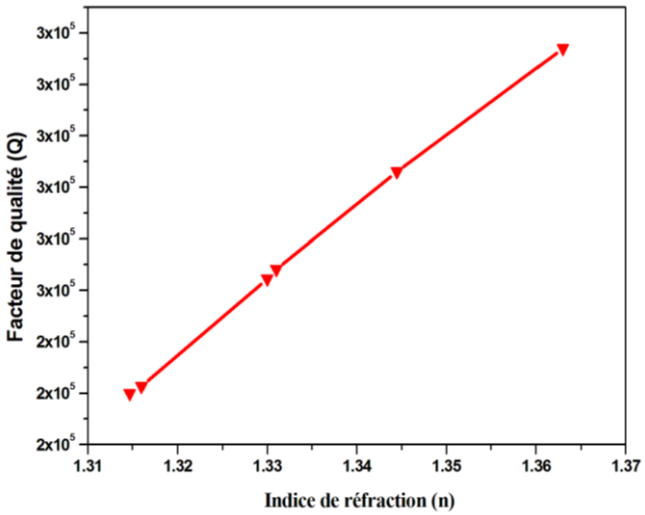

Figure 4. the Q factor variations according to the change of RI.

Note in the figure above that the quality factor Q increases with the increase in the refractive index.

Table 1. Biosensor sensitivity optimized for different liquids

Liquide	Indice de réfraction	Sensitivity (nm/RIU)	Δn(RIU)
L'eau distillée	1.3147	554.9	0.0153
Méthanol	1.316	554.29	0.014
L'eau déionisée	1.33	-	n_0
Analyte	1.331	550	0.001
Acétone	1.3445	553.1	0.0145
Alcool isopropylique	1.363	551.52	0.033

Table 2. Comparison of performance's parameters of the proposed biosensor with various similar PC-based designs.

Références	Type du capteur	Sensibilité (nm/RIU)	Δn
[22]2008	biocapteur RI formé de deux guides d'ondes et une microcavité	330	0,001
[23]2011	Capteurs RI à base de guide d'onde à CP	240	-
[24]2011	Capteurs RI à base de guide d'onde à CP	200	0,0014
[25]2012	Capteurs à base de cavité L3 à CP	35	0,038
[26]2013	Biocapteurs RI à base de guided'onde à CP	260	0,001
[27]2015	biocapteur RI formé de deux guides d'ondes et une microcavité	425	0,001
[28]2017	biocapteur RI formé de deux guides d'ondes et une microcavité		
Notre travail 2020	Design of high sensitive glucose concentration sensor based on ring-shaped holes photonic crystal cavity	550	0,001

The spectral response of the cavity as a function of changes in the refractive index, corresponding to the infiltration of the aqueous solution with the seven cases of glucose concentration is shown in the following figure:

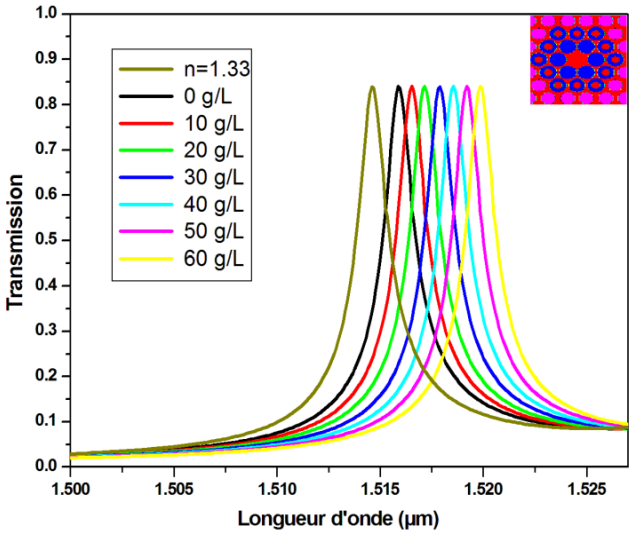

Figure 4. Normalized transmission spectrum of the PC microcavity as a function of wavelength .

The resonance peak located at 1514.6 nm ($a / \lambda = 0.363$) is identified as a reference mode corresponding to 0 g/l of glucose concentration. It should be noted that as the glucose concentration increases, the cavity mode shifts in response to the increase in refractive index from 1.33230545 to 1.33943885.

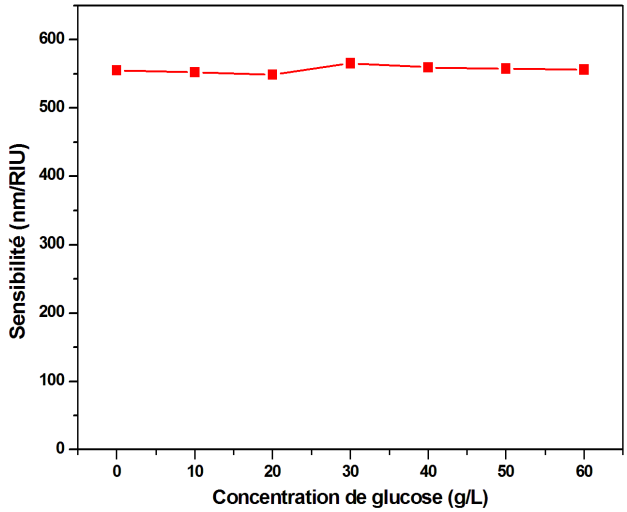

Figure 5. The S variations according to the change of the glucose concentration.

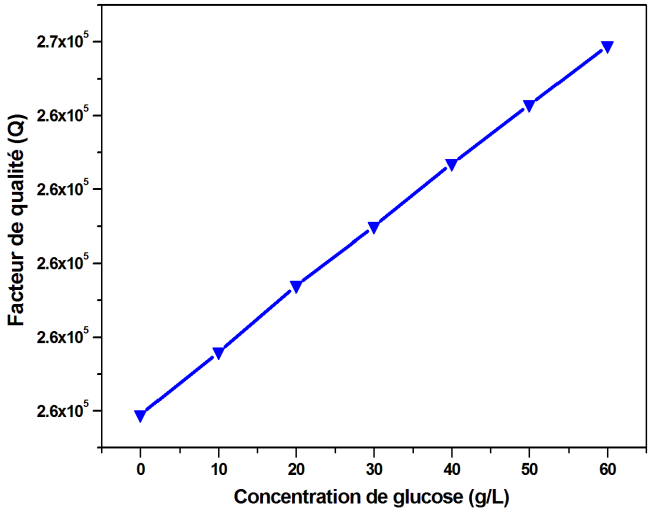

Figure 6. The Q factor variations according to the change of the glucose concentration.

As shown in figures (5 and 6), the sensitivity and the quality factor increase by increasing the glucose concentration (0 g/l - 60 g/l).

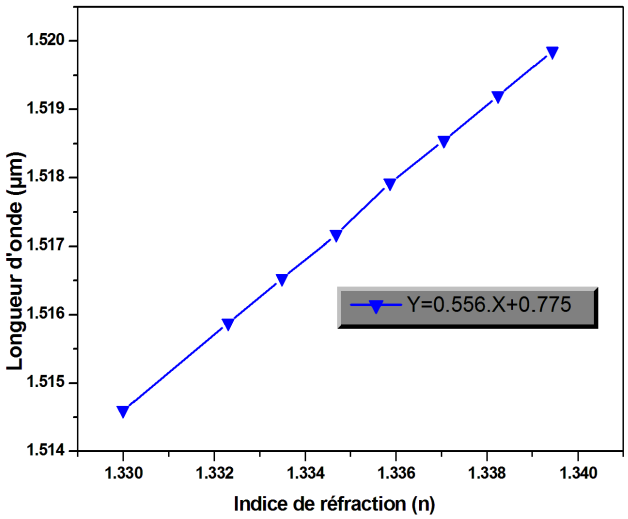

Figure 7. Resonant wavelength shift as a function of the RI n.

From figure 7, and if we assume that the relationship between the resonance shift and the refractive index is approximately linear, equation 8 describes the resonance displacement for a given liquid index to predict the resonant frequency after a linear fit of the simulation data:

$$Y[\mu m] = (0.556.x + 0.775)[\mu m] \quad (8)$$

Table 3. Comparison of performance's parameters of the proposed biosensor with various similar PC-based designs.

Référence	Structure de détection	S(nm/RIU)	Q	DL(RIU)
[22] 2008	Biocapteur formé par deux guides d'ondes et unemicrocavité.	330	$3{,}82\times10^{3}$	_
[30] 2017	Biocapteur constitué d'une nanocavité de type H2 et d'un guide d'onde W1à large bande.	131,70	$2{,}96\times10^{3}$	_
[22] 2008	Capteur à base de cavité à fente annulaire couplée à desguides d'ondes d'entrée et de sortie.	160	10^{7}	$8{,}75\times10^{-5}$
[29] 2014	Capteur constitué d'une cavité résonnante en forme d'anneau couplée à des guides d'ondes d'entrée et de sortie.	330	$8{,}2\times10^{6}$	$1{,}24\times10^{-5}$
[28] 2012	Capteur consistant en une cavité en anneau couplée à unguide d'onde optofluidique à lumière lente.	293	950	_
[31] 2017	Biocapteur basé sur un couplage d'une cavité de trous enforme d'anneau et de deux guides d'ondes d'entrée et desortie	462,61	$1{,}112\times10^{5}$	$3{,}03\times10^{-6}$
Dans ce travail 2021	Biocapteur basé sur un couplage d'une cavité de trous en forme losange et de deux guides d'ondes d'entrée et de sortie	520,5	$3{,}247\times10^{6}$	$8{,}99\times10^{-7}$
	Structure avec deux fonctions	**565,38**	**$2{,}610\times10^{5}$**	**$1{,}03\times10^{-6}$**

4. Conclusions

This work presents a new design for a PC-based cavity. The device structure consisted of two waveguides (input and output) in a 2-D-PC-Si-based layer, with a triangular lattice rhombus-shaped air holes. For the PC-based rhombus-shaped holes PC-RSH cavity, it has been demonstrated that a change in the RI of the rhombus contents corresponds to an increase in the glucose's concentration analyte. The variation in this latter is analyzed by using the FDTD method embedded in the commercial simulator RSoft. Various sensitivities of 565.38 nm/RIU and quality factor as high as 2.61×105have been accomplished, deducing in a location breaking points 1.03×10^{-6}. have been attained, respectively. Our proposed design with its four basic Structure of the proposed RI biosensor (sensor with two functions) can be implemented and used in many applications in the detection process of organisms and is a potential candidate for nanoscale sensors and so on.

5. References

[1]. Liedberg B, Lundström Iand Stenberg E 1993 *Sensors and Actuators B. Chemical.J.***11**6372

[2]. HeidemanRG,Lambeck PV 1999*Sens. Actuators B Chem.J.***61**100127

[3]. Scherer A, Painter O, Vuckovic J, Loncar MandYoshie T. 2002 *IEEE Transactions On Nanotechnology.J.***8** 411.

[4]. Mortensen N A, Xiao Sand Pedersen J 2007 *Microfluidics and Nanofluidics*. *J.***4** 117127

[5]. Caër C,Serna-Otálvaro S F,Zhang W,Le Roux XandCassan E2014*Opt. Lett.J.***39**57925794
[6]. Benmerkhi A,Bouchemat MandBouchemat T 2016*Optik. J.***127**56825687
[7]. Hocini A,Moukhtari R,Khedrouche D,Kahlouche AandZamani M2017 *Opt. Commun.J.***384**111117
[8]. Dutta H S,Pal S,2013*Opt. Quantum Electron. J.***45** 907917
[9]. Bougriou F,Bouchemat T,Bouchemat MandParaire N2013*Eur. Phys.Appl. Phys.J.***62**11201
[10]. Zhang Y,Zhao Y,Wang Q2013*Sens. Actuators BChem.J.***184**179188
[11]. Lai W C,Chakravarty S,Wang X,Lin CandChen RT.2011*Opt. Lett. J.***36**984986
[12]. Harhouz A,Hocini A2015*Electromagn. Wave Appl. J.* **29** 659667
[13]. Hocini A,Harhouz A2016 *Nanophotonics. J.***10** 016007016010
[14]. Di Falco A,O'Faolain LandKrauss TF.2009*Appl.Phys. Lett. J.* **94**06350310635033
[15]. Säynätjoki A,Mulot M,Vynck K,Cassagne D,Ahopelto JandLipsanen H. 2008 *Nanostruct. Fundam. Appl. J.* **6** 4246
[16]. Qiu M2002*Appl.Phys. Lett.J.* **81**1163
[17]. Kafesaki M,Soukoulis CMandAgio M.2002 *applied physics. J.***96** 40334038
[18]. Dutta H S,Goyal A K,Pal S2014 *Nanophotonics.J.***8** 083088083088
[19]. RigamontiG,Bello V,MerloS 2018*Sensors . J.***18**603
[20]. Yeh YL2008 *Opt. Lasers Eng. J.* **46** 667670
[21]. Dorfner DF,Hurlimann T,ZabelT,Frandsen LH,AbstreiterGandFinley JJ2008*Appl.Phys. Lett. J.***93**. 181103181106
[22]. Faraon A,Englund D,Fushman I,Vučković J,Stolz NandPetroff P2007*Appl.Phys. Lett.J.***90**213110213113
[23]. Loncar M,Scherer A2004*Optical Microcavities*(World Scientific Publishing)
[24]. Zhou J,Tian H,Yang D,Liu Q and Ji Y 2014 *Opt. Commun.J.* **330**175183
[25]. Benmerkhi A,Bouchemat M andBouchemat T 2016 *Photonics Nanostruct.J.***20**717
[26]. Huang L,Tian H,Zhou J,Liu Q,Zhang P andJi Y2015*Opt. Commun.J.***335**7377
[27]. Arafa S,Bouchemat M,Bouchemat T,Benmerkhi A andHocini A2017*Opt. Commun.J.***384**93100
[28]. Benelarbi D, Bouchemat T and BouchematM2017*Opt Quant Electron.J.* **49** 347
[29]. Arafa S,Bouchemat M,Bouchemat TandBenmerkhiA2017*Optik.J.***131**4957
[30]. White I M,Fan X 2008*Opt. Express .J.***16**10201028
[31]. Dominguez-Juarez J L,Kozyreff GandMartorell J2011*Nat. Commun.J.***2** 18